ЖЭТФ, 2019, том 156, вып. 4 (10), стр. 700–706

TOPOLOGICAL SUPERFLUIDS

G. E. Volovik*

Low Temperature Laboratory, Aalto University
FI-00076, Aalto, Finland

Landau Institute for Theoretical Physics, Russian Academy of Sciences
142432, Chernogolovka, Moscow Region, Russia

Received April 4, 2019,
revised version April 4, 2019
Accepted for publication April 5, 2019

Contribution for the JETP special issue in honor of I. M. Khalatnikov's 100th anniversary

DOI: 10.1134/S0044451019100110

There are many topological faces of the superfluid phases of ^{3}He. These superfluids contain various topological defects and textures. The momentum space topology of these superfluids is also nontrivial, as well as the topology in the combined $(\mathbf{p}, \mathbf{r})$ phase space, giving rise to topologically protected Dirac, Weyl, and Majorana fermions living in bulk, on the surface, and within the topological objects. The nontrivial topology leads to different types of anomalies, which extend the Landau–Khalatnikov theory of superfluidity in many different directions.

Superfluid phases of ^{3}He discovered in 1972 [1] opened the new area of the application of topological methods to condensed matter systems. Due to the multi-component order parameter which characterizes the broken symmetries in these phases, there are many inhomogeneous objects — textures and defects in the order parameter field — which are protected by topology and are characterized by topological charges. Among them there are quantized vortices, skyrmions and merons, solitons and vortex sheets, monopoles and boojums, Alice strings, Kibble walls terminated by Alice strings, spin vortices with soliton tails, etc. Some of them have been experimentally identified [2–5], the others are still waiting for their creation and detection.

The real-space topology, which is responsible for the topological stability of textures and defects, has been later extended to the topology in momentum space, which governs the topologically protected properties of the ground state of these systems. This includes in particular the existence of the topologically stable nodes in the fermionic spectrum in bulk and/or on the surface of superfluids. It appeared that the superfluid phases of liquid ^{3}He serve as the clean examples of the topological matter, where the momentum-space topology plays an important role in the properties of these phases.

In bulk liquid ^{3}He, there are two topologically different superfluid phases, ^{3}He-A and ^{3}He-B [6]. One is the chiral superfluid ^{3}He-A with topologically protected Weyl points in the quasiparticle spectrum. In the vicinity of the Weyl points, quasiparticles obey the Weyl equation and behave as Weyl fermions, with all the accompanying effects such as chiral anomaly, chiral magnetic effect, chiral vortical effect, etc. The Adler–Bell–Jackiw equation, which describes the anomalous production of fermions from the vacuum, has been verified in experiments with skyrmions in ^{3}He-A [7]. Another phase is the fully gapped time reversal invariant superfluid ^{3}He-B. It has topologically protected gapless Majorana fermions living on the surface.

The polar phase of ^{3}He stabilized in ^{3}He confined in the nematically ordered aerogel [8] contains Dirac nodal ring in the fermionic spectrum.

The classification of the topological objects in the order parameter fields revealed the possibility of many configurations with nontrivial topology, which are described by the homotopy groups and by the relative homotopy groups. Some of the topological defects and topological textures are shown in Fig. 1.

All three superfluid phases discussed here are the spin-triplet p-wave superfluids, i. e., the Cooper pair has spin $S = 1$ and orbital momentum $L = 1$. The

* E-mail: volovik@boojum.hut.fi

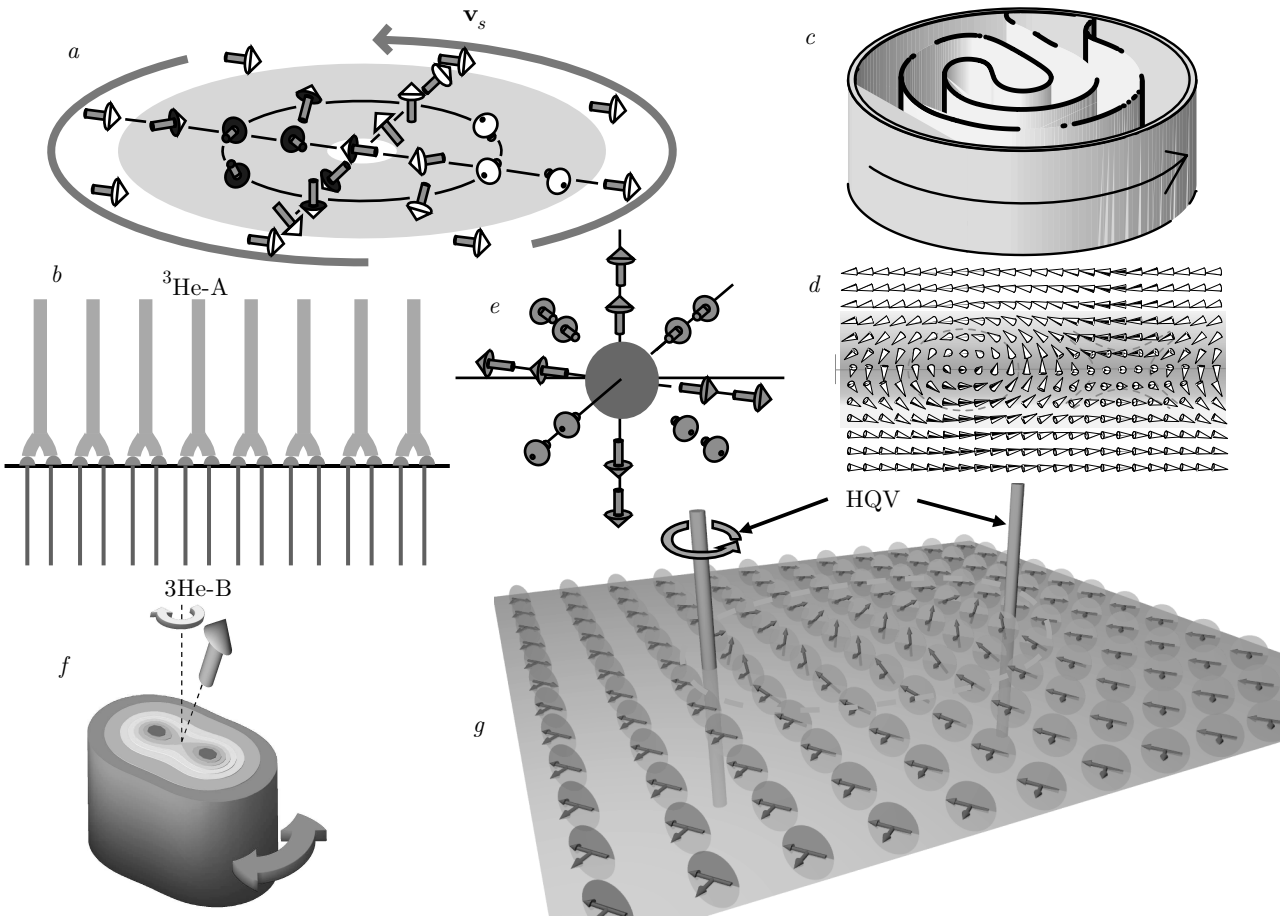

Fig. 1. (Color online) Some topological objects in topological superfluids. (*a*) Vortex-skyrmions with two quanta of circulation ($\mathcal{N} = 2$) in the chiral superfluid ^{3}He-A. (*b*) Interface between ^{3}He-A and ^{3}He-B in rotation: lattice of skyrmions with $\mathcal{N} = 2$ in ^{3}He-A transforms to the lattice of singly quantized vortices ($\mathcal{N} = 1$) in ^{3}He-B. Each skyrmion with $\mathcal{N} = 2$ splits into two merons with $\mathcal{N} = 1$ (Mermin – Ho vortices). The Mermin–Ho vortex terminates on the boojum — the surface singularity which is the analog of the Dirac monopole terminating the ^{3}He-B string (the $\mathcal{N} = 1$ vortex). (*c*) Vortex sheet in ^{3}He-A. (*d*) Elements of the vortex sheet: merons with $\mathcal{N} = 1$ within topological soliton in ^{3}He-A. (*e*) Hedgehog-monopole in the $\hat{\mathbf{d}}$-vector field in ^{3}He-A. (*f*) Singly quantized vortex ($\mathcal{N} = 1$) with spontaneously broken axial symmetry in ^{3}He-B as a pair of half-quantum vortices ($\mathcal{N} = 1/2$) connected by non-topological (dark) soliton. Such vortex has been identified due to Goldstone mode associated with the spontaneously broken axial symmetry of the vortex core — the twist oscillations of the vortex core propagating along the vortex line. This Figure is also applicable to the $\mathcal{N} = 2$ vortex in ^{3}He-B, which consists of two composite objects — spin-mass vortices connected by the topological soliton. (*g*) Half-quantum vortices (HQV) in the polar phase of ^{3}He, which in a tilted magnetic field are connected by the topological spin soliton. Red arrows show direction of magnetic field, and blue arrows show direction of spin-nematic vector $\hat{\mathbf{d}}$, which rotates by π around each half-quantum vortex

order parameter is given by 3×3 matrix $A_{\alpha i}$ (see below Eq. (11)), which transforms as a vector under $SO(3)_S$ spin rotations (first index) and as a vector under $SO(3)_L$ orbital rotations (second index). The order parameter $A_{\alpha i}$ comes as the bilinear combination of the fermionic opertators, $A_{\alpha i} \propto \langle \psi \sigma_\alpha \nabla_i \psi \rangle$, where σ_α are Pauli matrices for the nuclear spin of ^{3}He atom.

In the ground state of ^{3}He-A, the order parameter matrix has the form

$$A_{\alpha i} = \Delta_A e^{i\Phi} \hat{d}_\alpha (\hat{e}^i_1 + i\hat{e}^i_2), \quad \hat{\mathbf{l}} = \hat{\mathbf{e}}_1 \times \hat{\mathbf{e}}_2 \,, \qquad (1)$$

where $\hat{\mathbf{d}}$ is the unit vector of the anisotropy in the spin space due to spontaneous breaking of $SO(3)_S$ symmetry; $\hat{\mathbf{e}}_1$ and $\hat{\mathbf{e}}_2$ are mutually orthogonal unit vectors; and $\hat{\mathbf{l}}$ is the unit vector of the anisotropy in the orbital space due to spontaneous breaking of $SO(3)_L$ symmetry. The $\hat{\mathbf{l}}$-vector also shows the direction of the orbital angular momentum of the chiral superfluid, which emerges due to spontaneous breaking of time reversal symmetry.

In the chiral superfluid, the superfluid velocity $\mathbf{v}_{\rm s}$ of the chiral condensate is determined not only by the condensate phase Φ, but also by the orbital triad $\hat{\mathbf{e}}_1$, $\hat{\mathbf{e}}_2$, and $\hat{\mathbf{l}}$:

$$\mathbf{v}_{\rm s} = \frac{\hbar}{2m}\left(\nabla\Phi + \hat{\mathbf{e}}_1^i \nabla \hat{\mathbf{e}}_2^i\right) , \qquad (2)$$

where m is the mass of the ^{3}He atom. In non-chiral superfluids, the vorticity is presented in terms of the quantized singular vortices with the phase winding $\Delta\Phi = 2\pi\mathcal{N}$ around the vortex core. In chiral superfluid ^{3}He-A, the vorticity can be continuous. The continuous vorticity is represented by the texture of the unit vector $\hat{\mathbf{l}}$ according to the Mermi – Ho relation

$$\nabla \times \mathbf{v}_{\rm s} = \frac{\hbar}{4m} e_{ijk} \hat{l}_i \nabla \hat{l}_j \times \nabla \hat{l}_k \, . \qquad (3)$$

Vorticity is created in the rotating cryostat. In ^{3}He-A, the continuous textures are more easily created than the singular objects with the hard core of the coherence length size ξ, which formation requires overcoming of large energy barrier. That is why the typical object which appears under rotation of cryostat with ^{3}He-A is the vortex-skyrmion. It is the continuous texture of the orbital $\hat{\mathbf{l}}$-vector in Fig. 1*a* without any singularity in the order parameter fields. This texture represents the vortex with doubly quantized ($\mathcal{N} = 2$) circulation of superfluid velocity around the texture, $\oint d\mathbf{r} \cdot \mathbf{v}_s = \mathcal{N}\kappa$, where $\kappa = h/2m$ is the quantum of circulation. The vortex-skyrmions have been identified in rotating cryostat in 1983. They are described by two topological invariants, in terms of the orbital vector $\hat{\mathbf{l}}$ and in terms of the spin nematic vector $\hat{\mathbf{d}}$:

$$m_l = \frac{1}{4\pi}\int dx\, dy\, \hat{\mathbf{l}} \cdot \left(\frac{\partial \hat{\mathbf{l}}}{\partial x} \times \frac{\partial \hat{\mathbf{l}}}{\partial y}\right) = \frac{1}{2}\mathcal{N} \, , \qquad (4)$$

$$m_d = \frac{1}{4\pi}\int dx\, dy\, \hat{\mathbf{d}} \cdot \left(\frac{\partial \hat{\mathbf{d}}}{\partial x} \times \frac{\partial \hat{\mathbf{d}}}{\partial y}\right) . \qquad (5)$$

In a high magnetic field, the vortex lattice consists of isolated vortex-skyrmions with $\mathcal{N} = 2$, $m_l = 1$, and $m_d = 0$. In the low field, when the magnetic energy is smaller than the spin-orbit interaction, the vortex-skyrmion with $m_d = m_l = 1$ becomes more preferable. The first order topological transition, at which the topological charge m_d of the skyrmion changes from 0 to 1, has been observed in acoustic experiments. In 1994, new type of continuous vorticity has been observed in ^{3}He-A: the vortex texture in the form of the vortex sheet, the topological soliton with kinks, the Mermin–Ho vortices with $\mathcal{N} = 1$ (Fig. 1*d*).

In addition to continuous vortex textures, the rotating state of ^{3}He-A may consist of the singular vortices with $\mathcal{N} = 1$ and the half-quantum vortices with $\mathcal{N} = 1/2$ — the condensed matter analogs of the Alice string in particle physics, in which $\hat{\mathbf{d}}$ changes sign when circling around the vortex:

$$\hat{\mathbf{d}}(\hat{\mathbf{r}}) e^{i\Phi(\hat{\mathbf{r}})} = \left(\hat{\mathbf{x}}\cos\frac{\phi}{2} + \hat{\mathbf{y}}\sin\frac{\phi}{2}\right) e^{i\phi/2} . \qquad (6)$$

When the azimuthal coordinate ϕ changes from 0 to 2π along the circle around this object, the vector $\hat{\mathbf{d}}(\hat{\mathbf{r}})$ changes sign and simultaneously the phase Φ changes by π, giving rise to $\mathcal{N} = 1/2$. The half-quantum vortices have been stabilized only recently and in a different phase — in the polar phase of ^{3}He confined in aerogel [4].

In the ground state of ^{3}He-B, the order parameter matrix has the form

$$A_{\alpha i} = \Delta_B e^{i\Phi} R_{\alpha i} \, , \qquad (7)$$

where $R_{\alpha i}$ is the real matrix of rotation, $R_{\alpha i} R_{\alpha j} = \delta_{ij}$. Vorticity in the non-chiral superfluid is always singular, but it is also presented in several forms. Even the $\mathcal{N} = 1$ vortex, where $\Phi(\hat{\mathbf{r}}) = \phi$, has an unusual structure of the singular vortex core. The first order phase transition has been observed, at which the vortex core becomes non-axisymmetric, i. e., the axial symmetry of the vortex is spontaneously broken in the vortex core. The Goldstone mode associated with this symmetry breaking was experimentally identified. On the other side of the transition, at high pressure, the structure of the vortex core in ^{3}He-B is axisymmetric, but it is also nontrivial. In the core, the discrete symmetry is spontaneously broken. As a result, the core does not contain the normal liquid, but is occupied by the chiral superfluid — the A-phase of ^{3}He. The phenomenon of the additional symmetry breaking in the core of the topological defect has been also discussed for cosmic strings — the so-called Witten string.

In the ground state of the polar phase, the order parameter matrix has the form

$$A_{\alpha i} = \Delta_P e^{i\Phi} \hat{d}_\alpha \hat{z}^i \, , \qquad (8)$$

where axis z is along the nafen strands. Topology of polar phase in nafen suggests existence of the half-quantum vortices, which have been observed in the NMR experiments. Fig. 1*g* shows a pair of half-quantum vortices in transverse magnetic field (red arrows).

Later it was found that the half-quantum vortices survive the phase transition to ^{3}He-B, where the half-quantum vortex is topologically unstable. In the B-phase, the half-quantum vortices pinned by the strands of nafen become the termination lines of the

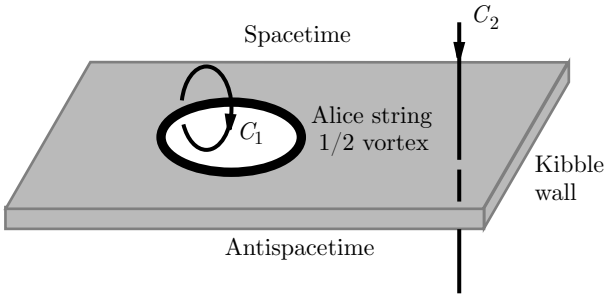

Fig. 2. (Color online) In ^{3}He-B, the half-quantum vortex (analog of Alice string) looses its topological stability and becomes the termination line of a non-topological domain wall — the Kibble wall [5]. In terms of the tetrads, the Kibble wall separates the states with different tetrad determinant, and thus between the "spacetime" and "antispacetime". There are two roads to antispacetime: the "safe" route around the Alice string (along the contour C_1) or "dangerous" route along C_2 across the Kibble wall

non-topological domain walls — the analog of Kibble cosmic walls [5]. In ^{3}He-B, the Kibble wall separates the states with different tetrad determinant, and thus separates the "spacetime" and "antispacetime", see Fig.2.

The topological stability of the coordinate dependent objects — defects and textures — is determined by the pattern of the symmetry breaking in these superfluids. Now we shall discuss these three phases of superfluid ^{3}He from the point of view of momentum-space topology, which describes the topological properties of the homogeneous ground state of the superfluids. These superfluids represent three types of topological materials, with different geometries of the topologically protected nodes in the spectrum of fermionic quasiparticles: Weyl points in ^{3}He-A, Dirac lines in the polar phase, and Majorana nodes on the surface of ^{3}He-B.

The properties of the fermionic spectrum in the bulk or/and on the surface of superfluids are determined by the topological properties of the Bogoliubov – de Gennes Hamiltonian

$$H(\mathbf{p}) = \begin{pmatrix} \epsilon(\mathbf{p}) & \hat{\Delta}(\mathbf{p}) \\ \hat{\Delta}^+(\mathbf{p}) & -\epsilon(\mathbf{p}) \end{pmatrix}, \quad \epsilon(\mathbf{p}) = \frac{p^2 - p_F^2}{2m^*}, \quad (9)$$

or by the Green's function

$$G^{-1}(\omega, \mathbf{p}) = i\omega - H\,. \quad (10)$$

For the spin triplet p-wave superfluid ^{3}He, the gap function is expressed in terms of the 3×3 order parameter matrix $A_{\alpha i}$:

$$\hat{\Delta}(\mathbf{p}) = A_{\alpha i}\sigma_\alpha \frac{p_i}{p_F}. \quad (11)$$

The topologically stable singularities of the Hamiltonian or of the Green's function in the momentum or momentum–frequency spaces look similar to the real-space topology of the defects and textures, see Fig. 3. The Fermi surface, which describes the normal liquid ^{3}He and metals, represents the topologically stable 2D object in the 4D frequency–momentum space (p_x, p_y, p_z, ω), is analogous to the vortex ring. The Weyl point in ^{3}He-A represents the topologically stable hedgehog in the 3D **p**-space, Fig. 3*b*. The Dirac nodal line in the polar phase of ^{3}He is the **p**-space analog of the spin vortex, Fig. 3*c*. The nodeless 2D systems (thin films of ^{3}He-A and the planar phase) and the nodeless 3D system — ^{3}He-B — are characterized by the topologically nontrivial skyrmions in momentum space in Fig. 3*e*.

The normal state of liquid ^{3}He belongs to the class of Fermi liquids, which properties at low energy are determined by quasiparticles living in the vicinity of the Fermi surface. The systems with Fermi surface, such as metals, are the most widespread topological materials in nature. The reason for that is that the Fermi surface is topologically protected and thus is robust to small perturbations. This can be seen on the simple example of the Green's function for the Fermi gas at the imaginary frequency:

$$G^{-1}(\omega, \mathbf{p}) = i\omega - \left(\frac{p^2}{2m} - \mu\right). \quad (12)$$

The Fermi surface at $p = p_F$ exists at positive chemical potential, with $p_F^2/2m = \mu$. The topological protection is demonstrated in Fig. 3*a* for the case of the 2D Fermi gas, where the Fermi surface is the line $p = p_F$ in (p_x, p_y)-space. In the extended (ω, p_x, p_y)-space, this gives rise to a singularity in the Green's function on the line at which $\omega = 0$ and $p = p_F$, where the Green's function is not determined. Such singular line in momentum–frequency space looks similar to the vortex line in real space: the phase $\Phi(\mathbf{p}, \omega)$ of the Green's function

$$G(\mathbf{p}, \omega) = |G(\mathbf{p}, \omega)|e^{i\Phi(\mathbf{p},\omega)}$$

changes by 2π around this line. In general, when the Green's function is the matrix with spin or/and band indices, the integer valued topological invariant — the winding number of the Fermi surface — has the following form:

$$N = \mathrm{Tr} \oint\limits_C \frac{dl}{2\pi i}\, G(\omega, \mathbf{p})\, \partial_l G^{-1}(\omega, \mathbf{p}). \quad (13)$$

Here, the integral is taken over an arbitrary contour C around the Green's function singularity in the $D + 1$

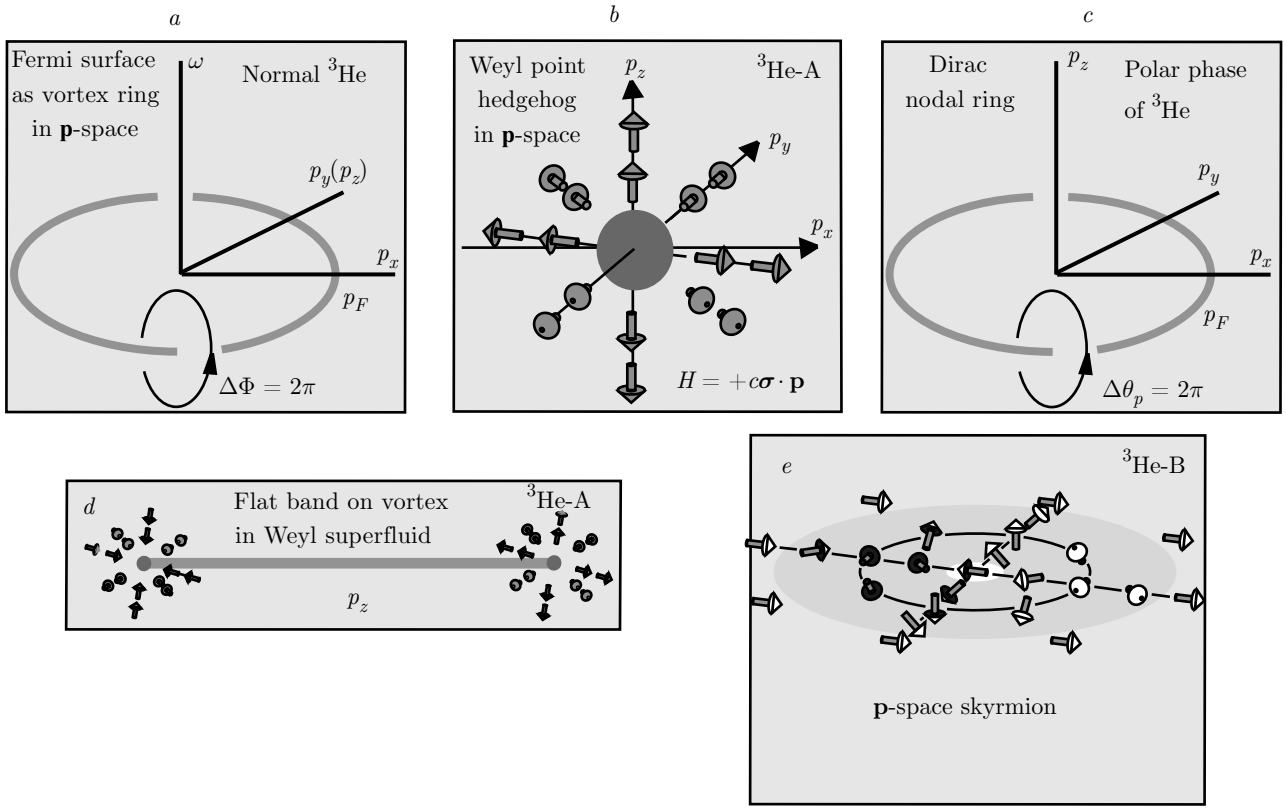

Fig. 3. Topological materials as configurations in momentum space. (a) Fermi surface in normal liquid ^{3}He is topologically protected, since the Green's function has singularity in the form of the vortex ring in the $(\mathbf{p},\omega)$-space. (b) Weyl point in ^{3}He-A as the hedgehog in $\mathbf{p}$-space. It can be also reperesented as the $\mathbf{p}$-space Dirac monopole with the Berry magnetic flux. (c) The polar phase has the Dirac nodal line in $\mathbf{p}$-space – the counterpart of the spin vortex in real space. (d) The $\mathcal{N} = \infty$ singular vortex in chiral superfluid ^{3}He-A has the 1D flat band terminated by the projections of the Weyl points to the vortex line. In real space it has analogy with the Dirac monopole terminating the Dirac string. (e) Skyrmion configurations in $\mathbf{p}$-space describe the fully gapped topological superfluids. The 2D skyrmion describes the topology of the ^{3}He-A state in a thin film and the topology of 2D planar phase of ^{3}He. The 3D $\mathbf{p}$-space skyrmion describes the superluid ^{3}He-B

momentum–frequency space. Due to nontrivial topological invariant, Fermi surface survives the perturbative interaction and exists in the Fermi liquid as well. Moreover, the singularity in the Green's function remains if due to interaction the Green's function has no poles, and thus quasiparticles are not well defined. The systems without poles include the marginal Fermi liquid, Luttinger liquid, and the Mott pesudogap state.

Under the superfluid transition, the 2×2 matrix of the normal liquid Green's function with spin indices transforms to the 4×4 Gor'kov Green's function. The simplified Green's function, which describes the topology of the chiral superfluid ^{3}He-A, has the form

$$G^{-1} = i\omega + \tau_3\left(\frac{p^2}{2m} - \mu\right) + \\ + c(\boldsymbol{\sigma}\cdot\hat{\mathbf{d}})\left(\tau_1\hat{\mathbf{e}}_1\cdot\mathbf{p} + \tau_2\hat{\mathbf{e}}_2\cdot\mathbf{p}\right). \quad (14)$$

The Pauli matrices $\tau_{1,2,3}$ and $\sigma_{x,y,z}$ correspond to the Bogoliubov–Nambu spin and ordinary spin of ^{3}He atom, respectively; and the parameter $c = \Delta_A/p_F$.

Now, there are two points in the fermionic spectrum, at $\mathbf{K}_\pm = \pm p_F\hat{\mathbf{l}}$, where the energy spectrum is nullified and the Green's function is not determined at $\omega = 0$. There are several ways of how to describe the topological protection of these two points. In terms of the Green's function, there is the following topological invariant expressed via integer valued integral over the 3D surface σ around the singular point in the 4-momentum space $p_\mu = (\omega, \mathbf{p})$:

$$N = \frac{e_{\alpha\beta\mu\nu}}{24\pi^2}\times \\ \times \mathrm{Tr}\int\limits_\sigma dS^\alpha\, G\partial_{p_\beta}G^{-1}G\partial_{p_\mu}G^{-1}G\partial_{p_\nu}G^{-1}. \quad (15)$$

If the invariant (15) is nonzero, the Green's function has a singularity inside the surface σ, and this means that fermions are gapless. The typical singularities have topological charge $N = +1$ or $N = -1$. Close to such points, the quasiparticles behave as right-handed and left-handed Weyl fermions, respectively, that is why such point node in the spectrum is called the Weyl point. The isolated Weyl point is protected by topological invariant (15) and survives when the interaction between quasiparticles is taken into account.

In ^{3}He-A, the topological invariants of the points at $\mathbf{K}^{(a)} = \pm k_F \hat{\mathbf{l}}$ are correspondingly $N = +2$ and $N = -2$: the Weyl points are degenerate over the spin of the ^{3}He atoms. Considering only single spin projection one comes to the 2×2 Bogoluibov–Nambu Hamiltonian for the spinless fermions:

$$H = \boldsymbol{\tau} \cdot \mathbf{g}(\mathbf{p}) \,, \tag{16}$$

where the vector function $\mathbf{g}(\mathbf{p})$ has the following components in ^{3}He-A:

$$g_1 = \hat{\mathbf{e}}_1 \cdot \mathbf{p}, \quad g_2 = \hat{\mathbf{e}}_2 \cdot \mathbf{p}, \quad g_3 = \frac{p^2}{2m} - \mu \,. \tag{17}$$

The Hamiltonian (16) is nullified at two points $\mathbf{K}^{(a)} = \pm p_F \hat{\mathbf{l}}$, where $p = p_F$ and $\mathbf{p} \cdot \hat{\mathbf{e}}_1 = \mathbf{p} \cdot \hat{\mathbf{e}}_2 = 0$. At these points the unit vector $\hat{\mathbf{g}}(\mathbf{p}) = \mathbf{g}(\mathbf{p})/|\mathbf{g}(\mathbf{p})|$ has the singularity of the hedgehog-monopole type in Fig. 3*b*, which is described by the dimensional reduction of the invariant (15):

$$N = \frac{1}{8\pi} e_{ikl} \int\limits_{\sigma} dS^i \, \hat{\mathbf{g}} \cdot \left(\frac{\partial \hat{\mathbf{g}}}{\partial p_k} \times \frac{\partial \hat{\mathbf{g}}}{\partial p_l} \right) , \tag{18}$$

where σ now is the 2D spherical surface around the hedghehog.

The hedgehog has $N = \pm 1$ and it represents the Berry phase magnetic monopole in terms of the deviation of the momentum $\mathbf{p}$ from the Weyl point at $\mathbf{K}^{(a)}$:

$$H^{(a)} = e^i_\alpha \tau^\alpha (p_i - K^{(a)}_i) + \dots \tag{19}$$

Introducing the effective electromagnetic field $\mathbf{A}(\mathbf{r}, t) = p_F \hat{\mathbf{l}}(\mathbf{r}, t)$ and effective electric charge $q^{(a)} = \pm 1$, one obtains

$$H^{(a)} = e^i_\alpha \tau^\alpha (p_i - q^{(a)} A_i) + \dots \tag{20}$$

Such Hamiltonian decsribes the Weyl fermions moving in the effective electric and magnetic fields

$$\mathbf{E}_{eff} = -p_F \partial_t \hat{\mathbf{l}}, \quad \mathbf{B}_{eff} = p_F \nabla \times \hat{\mathbf{l}} \,, \tag{21}$$

and also in the effective gravitational field represented by the triad field $e^i_\alpha(\mathbf{r}, t)$. The effective quantum electrodynamics emerging in the vicinity of the Weyl point leads to many analogs in relativistic quantum field theories, including the zero charge effect — the "Moscow zero" by Abrikosov, Khalatnikov, and Landau [9].

In the polar phase of ^{3}He, the simplified Hamiltonian is

$$H = \tau_3 \left(\frac{p^2}{2m} - \mu \right) + c p_z (\boldsymbol{\sigma} \cdot \hat{\mathbf{d}}) \tau_1 \,. \tag{22}$$

It is nullified when $p_z = 0$ and $p_x^2 + p_y^2 = p_F^2$, i. e., the spectrum of quasiparticles has the nodal line in Fig. 3*c*. The nodal line is protected by topology due to the discrete symmetry: the Hamiltonian (22) anticommutes with τ_2, which allows us to write the topological charge:

$$N = \mathrm{Tr} \oint\limits_C \frac{dl}{4\pi i} \, \tau_2 H^{-1}(\mathbf{p}) \, \partial_l H(\mathbf{p}) \,. \tag{23}$$

Here, C is an infinitesimal contour in momentum space around the line, which is called the Dirac line. The topological charge N in Eq. (23) is integer and is equal to 2 for the nodal line in the polar phase due to spin degeneracy.

^{3}He-B belongs to the same topological class as the vacuum of Standard Model in its present insulating phase. The topological classes of the ^{3}He-B states can be represented by the simplified Bogoliubov – de Gennes Hamiltonian

$$\begin{gathered} H = \tau_3 \left(\frac{p^2}{2m} - \mu \right) + \tau_1 \Delta_B \boldsymbol{\sigma} \cdot \hat{\mathbf{d}}(\mathbf{p}), \\ \hat{d}_\alpha(\mathbf{p}) = \pm R_{\alpha i} \frac{p_i}{p_F} \,. \end{gathered} \tag{24}$$

Here, $R_{\alpha i}$ is the matrix of rotation; the phase of the order parameter in Eq. (7) is chosen either $\Phi = 0$ or $\Phi = \pi$. There are no nodes in the spectrum of fermions: the system is fully gapped. Nevertheless, ^{3}He-B is the topological superfluid, which can be seen from the integer valued integral over the former Fermi surface:

$$N_d = \frac{1}{8\pi} e_{ikl} \int\limits_{S^2} dS^i \, \hat{\mathbf{d}} \cdot \left(\frac{\partial \hat{\mathbf{d}}}{\partial p_k} \times \frac{\partial \hat{\mathbf{d}}}{\partial p_l} \right) , \tag{25}$$

where $N_d = \pm$ depending on the sign in Eq. (24).

In terms of the Hamiltonian, the topological invariant can be written as integral over the whole momentum space (or over the Brillouin zone in solids)

$$\begin{aligned} N_K = {} & \frac{e_{ijk}}{24\pi^2} \times \\ & \times \mathrm{Tr} \left[\int d^3p \, K H^{-1} \partial_{p_i} H H^{-1} \partial_{p_j} H H^{-1} \partial_{p_k} H \right] , \end{aligned} \tag{26}$$

where $K = \tau_2$ is the matrix which anticommutes with the Hamiltonian. One has $N_K = 2N_d$ due to spin degrees of freedom.

The nontrivial topology of ^{3}He superfluids leads to the topologically protected massless (gapless) Majorana fermions living on the surface of the superfluid or/and inside the vortex core.

In conclusion, at the moment the known phases of liquid ^{3}He belong to 4 different topological classes.

(i) The normal liquid ^{3}He belongs to the class of systems with topologically protected Fermi surfaces. The Fermi surface is described by the first odd Chern number in terms of the Green's function in Eq. (13).

(ii) Superfluid ^{3}He-A and ^{3}He-A$_1$ are chiral superfluids with the Majorana–Weyl fermions in bulk, which are protected by the Chern number in Eq. (15). In the relativistic quantum field theories, Weyl fermions give rise to the effect of chiral (axial) anomaly. The direct analog of this effect has been experimentally demonstrated in ^{3}He-A [7]. It is the first condensed matter, where the chiral anomaly effect has been observed.

The singly quantized vortices in superfluids with Weyl points contain dispersionless band (flat band) of Andreev–Majorana fermions in their cores [10].

The glass phases of this chiral superfluid have been observed in aerogel, see review [11]. Among them are the so-called Larkin–Imry–Ma states — the glass states of the $\hat{\mathbf{l}}$-field, which can be represented as disordered tangle of vortex skyrmions. The spin glass state in the $\hat{\mathbf{d}}$-field has been also observed. These are the first representatives of the inhomogeneous disordered ground state of the topological material.

(iii) ^{3}He-B is the purest example of a fully gapped superfluid with topologically protected gapless Majorana fermions on the surface. In magnetic field, this phase becomes the higher order topological superfluid.

(iv) The most recently discovered polar phase of superfluid ^{3}He belongs to the class of fermionic materials with topologically protected lines of nodes, and thus contains two-dimensional flat band of Andreev–Majorana fermions on the surface of the sample.

It is possible that with the properly engineered nanostructural confinement one may reach also new topological phases of liquid ^{3}He including the following.

(i) The planar phase, which is the non-chiral superfluid with Dirac nodes in the bulk and with Fermi arc of Andreev–Majorana fermions on the surface.

(ii) The 2D topological states in the ultra-thin film, including inhomogeneous phases of superfluid ^{3}He films. The films with the ^{3}He-A and the planar phase order parameters belong to the 2D fully gapped topological materials, which experience the quantum Hall effect and the spin quantum Hall effect in the absence of magnetic field.

(iii) α-state, which contains 4 left and 4 right Weyl points in the vertices of a cube [12]. This is close to the high energy physics model with 8 left-handed and 8 right-handed Weyl fermions in the vertices of a 4D cube. This is one of many examples when the topologically protected nodes in the spectrum serve as an inspiration for the construction of the relativistic quantum field theories.

Acknowledgements. This work has been supported by the European Research Council (ERC) under the European Union's Horizon 2020 research and innovation programme (Grant Agreement No. 694248).

The full text of this paper is published in the English version of JETP.

REFERENCES

1. D. D. Osheroff, R. C. Richardson, and D. M. Lee, Phys. Rev. Lett. **28**, 885 (1972).

2. M. M. Salomaa and G. E. Volovik, Rev. Mod. Phys. **59**, 533 (1987).

3. A. P. Finne, V. B. Eltsov, R. Hanninen, N. B. Kopnin, J. Kopu, M. Krusius, M. Tsubota, and G. E. Volovik, Rep. Progr. Phys. **69**, 3157 (2006).

4. S. Autti, V. V. Dmitriev, V. B. Eltsov, J. Makinen, G. E. Volovik, A. N. Yudin, and V. V. Zavjalov, Phys. Rev. Lett. **117**, 255301 (2016).

5. J. T. Mäkinen, V. V. Dmitriev, J. Nissinen, J. Rysti, G. E. Volovik, A. N. Yudin, K. Zhang, and V. B. Eltsov, Nature Comm. **10**, 237 (2019).

6. D. Vollhardt and P. Wölfle, *The Superfluid Phases of Helium 3*, Dover Publ., New York (2013).

7. T. D. C. Bevan, A. J. Manninen, J. B. Cook, J. R. Hook, H. E. Hall, T. Vacaspati, and G. E. Volovik, Nature **386**, 689 (1997).

8. V. V. Dmitriev, A. A. Senin, A. A. Soldatov, and A. N. Yudin, Phys. Rev. Lett. **115**, 165304 (2015).

9. L. D. Landau, A. A. Abrikosov, and I. M. Khalatnikov, Dokl. Akad. Nauk SSSR **95**, 497, 773, 1177 (1954).

10. N. B. Kopnin and M. M. Salomaa, Phys. Rev. B **44**, 9667 (1991).

11. G. E. Volovik, J. Rysti, J. T. Makinen, and V. B. Eltsov, J. Low Temp. Phys. **196**, 82 (2019).

12. G. E. Volovik and L. P. Gor'kov, Zh. Eksp. Teor. Fiz. **88**, 1412 (1985).